W physics in e^+e^-collisions at $\sqrt{s} = 161$ and 172 GeV at LEP

Takayuki Saeki
University of Tokyo, Bunkyo-ku, Tokyo 113, Japan

on behalf of the ALEPH, DELPHI, L3 and OPAL collaborations

In June 1996, the LEP center-of-mass energy was raised to 161 GeV, just above the threshold of pair-production of W bosons. ALEPH, DELPHI, L3, and OPAL detectors observed the pair-production of W bosons for the first time in e^+e^- collisions. In October the same year, the center-of-mass energy was raised to 172 GeV, significantly above the threshold. The four detectors collected data successfully at both energies. We present the results on W physics which cover the total cross section of the W boson pair-production, the W decay branching fractions, the measurements of the mass of the W boson, the triple gauge-boson couplings, and W pair-production properties. All the results are consistent with the Standard Model expectations.

I. INTRODUCTION

In June 1996, the LEP2 started with the center-of-mass energy (CME) of 161 GeV, just above the threshold of pair-production of W bosons. This allowed to observe and study the first W-pair production events through the four detectors, i.e. ALEPH, DELPHI, L3, and OPAL, in the very clear environment of e^+e^- collisions. Detailed descriptions of the four detectors can be found elsewhere [1–4]. The recorded data per experiment at this energy corresponds to an integrated luminosities of about 11 pb^{-1}. In October the same year, the CME was raised to 172 GeV, significantly above the threshold. The four detectors collected data successfully again and the integrated luminosity per experiment was about 11 pb^{-1}. This article presents main results on W-pair production obtained by the four experiments using these data.

II. SELECTION

WW events are produced through three doubly resonant diagrams (s-channel γ and Z^0 exchange and t-channel ν exchange), called "CC03 diagrams", where each W can decay into quark pair or lepton-nutorino pair. This leads to the classification of WW events into three channels, i.e. fully hadronic, semileptonic, and fully leptonic channels. WW events are selected with good efficiency and high purity in the analysis, utilising corresponding event-topology to the three channels.

A. Fully hadronic channel

The typical final state of the fully hadronic events is specified by four hadronic jets whose energy sum is consistent with the center-of-mass energy. Display for a typical fully hadronic WW event from OPAL is shown in Fig. 2, where

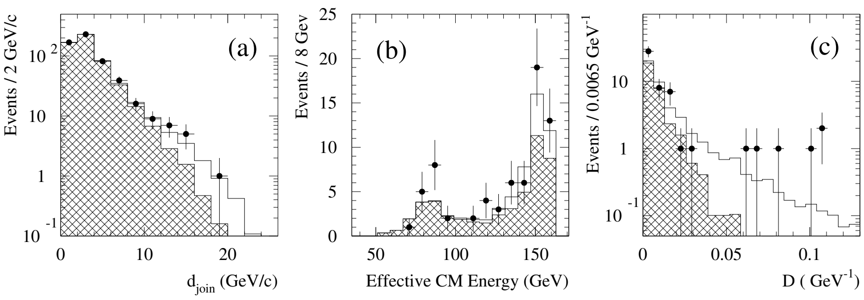

FIG. 1. Selection for fully hadronic final state from DELPHI: comparison of data (points) with background (hatched-area) and WW signal (white area). (a) Differential 3-jet rate as function of d_{join}; (b) effective CME for events with at least 4 jets; (c) D variable for 4-jet events with effective CME > 115 GeV.

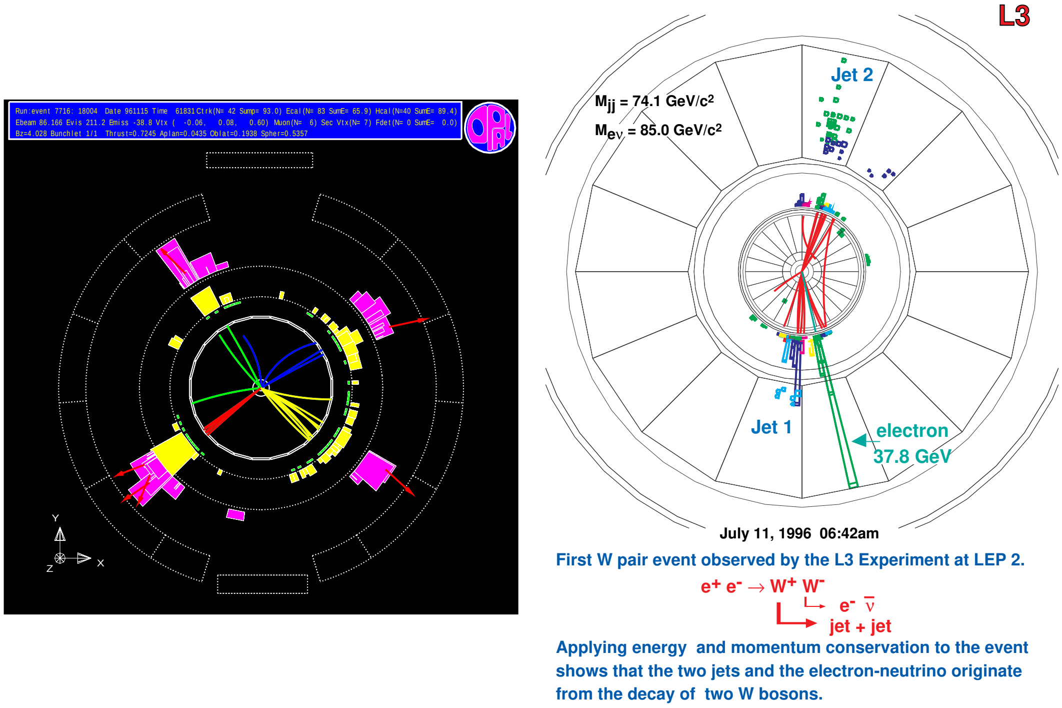

FIG. 2. Left-hand side: event display of typical fully hadronic WW event from OPAL. Right-hand side: event display of typical semileptonic WW event from L3.

four jets can be seen clearly. The event selection criteria were optimised in order to ensure that the final state was purely hadronic and in order to reduce the residual background. The background is dominated by electron-positron annihilation to $q\overline{q}(\gamma)$, with a cross-section about two orders of magnitude larger than that for signal. Here the selection criteria for DELPHI experiment at 161 GeV is described. For each event, all particles are clustered into jets using the LUCLUS algorithm [5] with $d_{join} = 6.5$ GeV/c. At least 4 jets are required, with at least four particles in each jet. Fig. 1a shows the distributions of the differential 3-jet rate as a function of d_{join} for data and simulated WW and background events.

Events coming from the radiative return Z peak are rejected by requiring the effective center-of-mass energy of e^+e^- annihilation to be larger than 115 GeV. The effective energy was estimated from the momentum of the radiative photon. Fig. 1b shows the distributions of the effective energy for events with at least 4 jets. Events are then forced into a 4-jet configuration, and a kinematically constrained fit performed, imposing energy and momentum conservation. The final cut is made on the variable

$$D = \frac{E_{min}\theta_{min}}{E_{max}(E_{max} - E_{min})}, \tag{1}$$

where E_{min}, E_{max} are the energies of the jets with least and greatest energy, and θ_{min} is the smallest interjet angle, after the constrained fit. D is required to exceed 0.013 GeV^{-1} and discriminates well between the signal and the $q\overline{q}(\gamma)$ background. Fig. 1c shows the distributions of D variable after the other two cuts described above. The selection efficiency was computed from a sample of WW Monte Carlo events, and found to be $(61.3 \pm 2.0)\%$.

At 172 GeV, the ratio of the signal cross-section to the cross-section of Z^0/γ events is about four times larger than at threshold. This allows some of the cuts to be relaxed and improves the efficiency of the selections. Other selection cuts are rescaled in accordance with the increase in total energy. The selection efficiency was estimated to be $(82.7 \pm 1.6)\%$ from Monte Carlo simulation. The residual cross-sections of $q\overline{q}(\gamma)$ events after these selection procedures at 161 and 172 GeV were estimated to be 0.58 and 1.96 pb, respectively.

B. Semileptonic channel

Semileptonic final states, $W^+W^- \to q\overline{q}\,l\overline{\nu}_l$, are expected to comprise 44% of W^+W^- decays. $W^+W^- \to q\overline{q}e\overline{\nu}_e$ and $W^+W^- \to q\overline{q}\mu\overline{\nu}_\mu$ events are characterised by two well-separated hadronic jets, a high momentum lepton and sizable

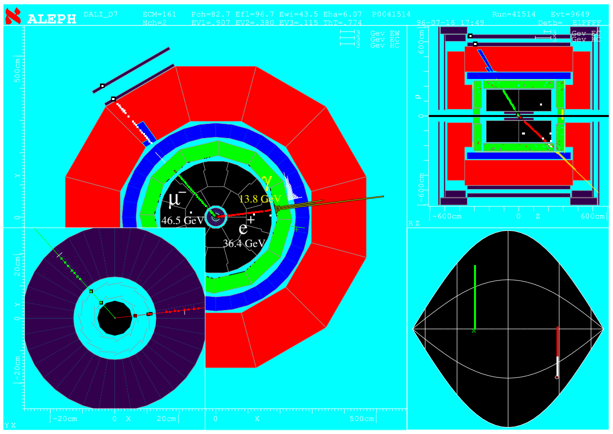

FIG. 3. Event display of typical fully leptonic WW event from ALEPH.

missing momentum due to the unobserved neutrino. Display for a typical semileptonic WW event from L3 is shown in Fig. 2, where two jets and one track for electron are seen. The signature for $W^+W^- \to q\overline{q}\tau\overline{\nu}_\tau$ events is two well separated jets from the hadronic W decay and one low multiplicity jet typically consisting of one or three tracks. The expected missing momentum is less well defined due to the additional neutrino(s) from the decay of the tau.

The selection criteria of $W^+W^- \to q\overline{q}\, l\overline{\nu}_l$ channel for OPAL experiment at 172 GeV are described here. The $W^+W^- \to q\overline{q}\, l\overline{\nu}_l$ event selection consists of three separate selections, one for each type of semileptonic decay. The $W^+W^- \to q\overline{q}\tau\overline{\nu}_\tau$ selection is applied only to events which fail the $W^+W^- \to q\overline{q}e\overline{\nu}_e$ and $W^+W^- \to q\overline{q}\mu\overline{\nu}_\mu$ selections. Each selection proceeds in four stages. Stage 1 is the identification of the candidate lepton. The track with the highest probability of being a lepton from either the decay $W \to e\overline{\nu}_e$ or $W \to \mu\overline{\nu}_\mu$ is identified. The $W^+W^- \to q\overline{q}\tau\overline{\nu}_\tau$ selection uses the track (or tracks) most consistent with being from a tau decay from $W^+W^- \to q\overline{q}\tau\overline{\nu}_\tau$. Stage 2 is the preselection. Cuts are applied to the data to reduce the background from $Z^0/\gamma \to q\overline{q}$ events. Stage 3 is the relative likelihood selection which, based on kinematic variables and the lepton candidate, are used to distinguish signal events ($W^+W^- \to q\overline{q}e\overline{\nu}_e$ $W^+W^- \to q\overline{q}\mu\overline{\nu}_\mu$ and $W^+W^- \to q\overline{q}\tau\overline{\nu}_\tau$) from $Z^0/\gamma \to q\overline{q}$ background events. Events passing the likelihood selection are considered to be $W^+W^- \to q\overline{q}\, l\overline{\nu}_l$ candidates. Stage 4 is the event categorisation. Having suppressed the background using the relative likelihood selection, a second relative likelihood is applied to the $W^+W^- \to q\overline{q}e\overline{\nu}_e$ and $W^+W^- \to q\overline{q}\mu\overline{\nu}_\mu$ candidates in order to categorise them as either $W^+W^- \to q\overline{q}e\overline{\nu}_e$, $W^+W^- \to q\overline{q}\mu\overline{\nu}_\mu$ or $W^+W^- \to q\overline{q}\tau\overline{\nu}_\tau$ events.

	Generated as		
Selected as	$W^+W^- \to q\overline{q}e\overline{\nu}_e$	$W^+W^- \to q\overline{q}\mu\overline{\nu}_\mu$	$W^+W^- \to q\overline{q}\tau\overline{\nu}_\tau$
$W^+W^- \to q\overline{q}e\overline{\nu}_e$	$85.1 \pm 0.9\%$	$0.1 \pm 0.1\%$	$3.9 \pm 0.3\%$
$W^+W^- \to q\overline{q}\mu\overline{\nu}_\mu$	$0.2 \pm 0.1\%$	$87.6 \pm 0.8\%$	$4.4 \pm 0.3\%$
$W^+W^- \to q\overline{q}\tau\overline{\nu}_\tau$	$4.7 \pm 0.5\%$	$5.2 \pm 0.5\%$	$61.4 \pm 1.2\%$

TABLE I. Selection efficiencies for the different $W^+W^- \to q\overline{q}\, l\overline{\nu}_l$ channels after event categorisation showing the cross contamination in each selection at 172 GeV. The efficiencies have been corrected for differences between data and Monte Carlo. The errors include both statistical and systematic uncertainties.

Table I shows the efficiencies of the selections for $W^+W^- \to q\overline{q}\, l\overline{\nu}_l$ events after categorisation into the different channels. These efficiencies include corrections which account for observed differences between the data and the Monte Carlo simulation. The uncertainties include both systematic and statistical contributions. Efficiency corrections and systematic errors arising from discrepancies between data and Monte Carlo simulation were determined by studying data and Monte Carlo "mixed events" formed by superposing LEP1 hadronic Z^0 decay events and single hemispheres from LEP1 events identified as Z^0 decays to charged lepton pairs.

C. Fully leptonic channel

The typical fully leptonic WW events consist of two acoplanar energetic leptons with significant missing energy in

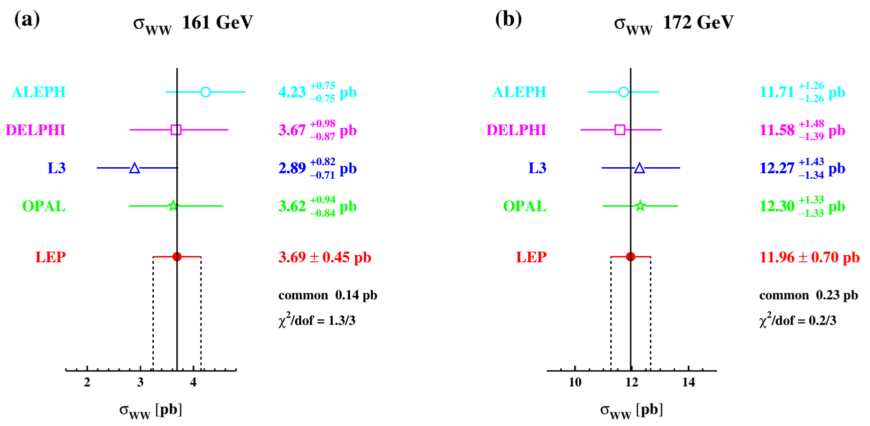

FIG. 4. The results of the W-pair cross-section measurements, (a) at 161 GeV and (b) at 172 GeV. Each error on the measured values is the quadratic sum of statistical and systematic uncertainties.

detectors. Display for a typical fully leptonic event from ALEPH is shown in Fig. 3, where two tracks for positron and muon can be seen. ALEPH developed two selections for the $W^+W^- \to l^+\nu l^-\overline{\nu}$ signal ($l = e, \mu$ or τ) for the threshold measurement. The two selections have overall efficiencies (62.7% and 66.9%) and background levels (0.038 pb and 0.028 pb). They have similar efficiencies and background levels, but differ in their sensitivities to the individual dilepton channels. The first analysis is based on topological information and is sensitive to all channels, where events are accepted if they contain two or four charged tracks with zero total electric charge. The second analysis requires from two to six charged tracks and the presence of at least one high momentum electron or muon. This leads to a comparatively lower efficiency (24% instead of 48%) for events where both Ws decay to tau, but the efficiency is higher in all other channels. Both analyses apply photon vetoes against radiative dilepton events. Events are accepted as WW candidates if they pass either of the two selections and the combined efficiency is 74% for a background of 0.053 pb. The two selections are also used in the analysis at 172 GeV without significant changes. They have the overall efficiencies (65% and 69%) and background levels (0.035 pb and 0.058 pb) at this energy, and the combined efficiency is 74% for a background of 0.065 pb. The residual background is dominated by $\gamma\gamma \to \tau\tau$ and non-CC03 four-fermion events at both energies. The largest detector related systematic effects come from the photon vetoes, with a systematic uncertainty of $\pm 2\%$. The overall systematic errors amount to ± 0.029 at 161 GeV and ± 0.07 at 172 GeV, and are dominated by Monte Carlo statistics.

III. DETERMINATION OF WW CROSS-SECTION

The numbers of WW events selected by four experiments are shown in Table II for each channel. We collected 117 and 467 WW candidates at 161 and 172 GeV, respectively, in total of four experiments.

	$W^+W^- \to q\overline{q}q\overline{q}$	$W^+W^- \to q\overline{q}\, l\overline{\nu}_l$	$W^+W^- \to l^+\nu l^-\overline{\nu}$	Total
ALEPH	16/65	16/44	6/10	38/119
DELPHI	15/65	12/45	2/8	29/118
L3	9/61	11/40	2/9	22/110
OPAL	14/57	12/55	2/8	28/120
Total	54/248	51/184	12/35	117/467

TABLE II. Number of WW candidates selected at 161/172 GeV.

W^+W^- production cross-section and branching fractions are measured by using likelihood method. For example, OPAL used the information from ten separate channels for these measurements. For each channel i, the probability of obtaining the number of observed events is calculated as a function of the W^+W^- cross-section, σ_{WW}, and the

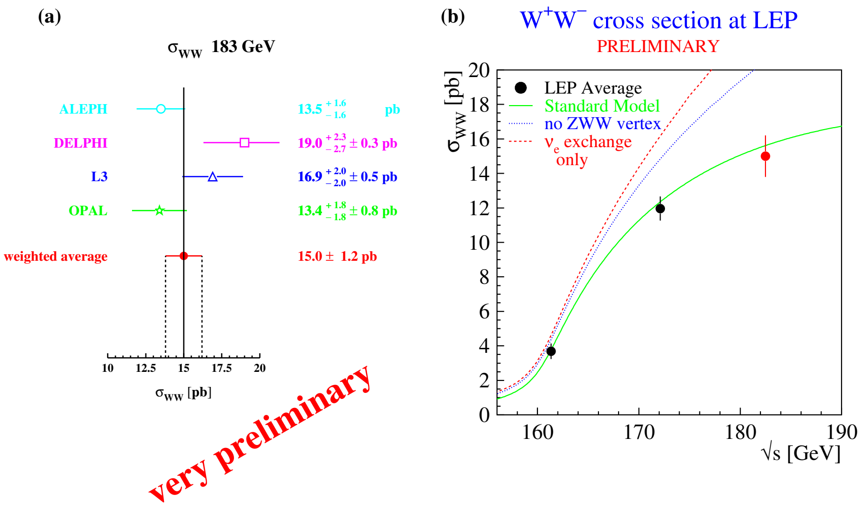

FIG. 5. (a) The W-pair cross-section at 183 GeV and (b) the W-pair cross-section as a function of the CME. The data points are the LEP averages. Also shown is the Standard Model prediction (solid line), and for comparison the cross-section if the ZWW coupling did not exist (dotted line), or if only the t-channel ν_e exchange diagram existed (dashed line).

W branching fractions, using Poisson statistics and assuming Standard Model branching ratios. The likelihood $\mathcal{L}$ is formed from the product of these Poisson probabilities $\mathcal{P}_i$, of observing N_i events for a Monte Carlo prediction of μ_i events:

$$\mathcal{L} = \prod_i \mathcal{P}_i(N_i, \mu_i) = \prod_i \frac{\mu_i^{N_i} \exp(-\mu_i)}{N_i!}. \tag{2}$$

If μ_i is given as a function of σ_{WW}, the maximum likelihood value yields the measurement of the CC03 cross-section. Fig. 4 (a) and (b) show results from four experiments at 161 and 172 GeV, respectively. Fig. 5 (a) shows preliminary result at 183 GeV and (b) shows the energy dependence of the $\mathrm{W}^+\mathrm{W}^-$ production cross-section. The data are seen to be consistent with the Standard Model.

If μ_i is the function of a W branching fraction, the maximum likelihood value yields the measurement of the corresponding W branching fraction. Fig. 6 shows results of W branching fractions from four experiments and the combined results, where (a) is for $\mathrm{W}\to\mathrm{q}\overline{\mathrm{q}}$ and (b) is for $\mathrm{W}\to l\overline{\nu}_l$. The hadronic branching ratio is determined assuming lepton universality.

IV. IMPROVEMENT ON CKM-MATRIX ELEMENT V_{CS}

This section describes an improvement on the measurement of the Cabibbo-Kobayashi-Maskawa (CKM) matrix elements V_{CS} by LEP2. Concerning measurements on CKM matrix elements by other experiments, apart from the elements describing the decays of the heavy t-quark, the value of the element relating the quarks of the second generation is known with poorest precision. The $|V_{\mathrm{CS}}|$ is measured to be 1.01 ± 0.18 in semileptonic decays of D mesons [6], where the absolute error of 18% is dominated by the poorly known hadronic form-factor. On the other hand, the nominal value of $|V_{\mathrm{CS}}| = 0.9394 \pm 0.0008$ can be determined from the CKM unitarity constraint [6].

Within the framework of the Standard Model, the W boson branching fractions depend on the six elements of the CKM mixing matrix, $|V_{ij}|$, which do not involve the top quark [7]

$$\frac{\mathrm{Br}(\mathrm{W}\to\mathrm{q}\overline{\mathrm{q}})}{(1-\mathrm{Br}(\mathrm{W}\to\mathrm{q}\overline{\mathrm{q}}))} = \left(1 + \frac{\alpha_s(M_{\mathrm{W}})}{\pi}\right) \sum_{i=\mathrm{u,c};\, j=\mathrm{d,s,b}} |V_{ij}|^2, \tag{3}$$

where $\alpha_s(M_{\mathrm{W}})$ is taken to be 0.118 ± 0.003 [6]. The effect of finite quark masses, m_q, on the W branching ratios are of order $(m_{\mathrm{q}}/M_{\mathrm{W}})^2$ [7], and are therefore neglected. The LEP combined result for the branching fraction $\mathrm{Br}(\mathrm{W}\to\mathrm{q}\overline{\mathrm{q}})$ obtained from the fit assuming lepton universality gives:

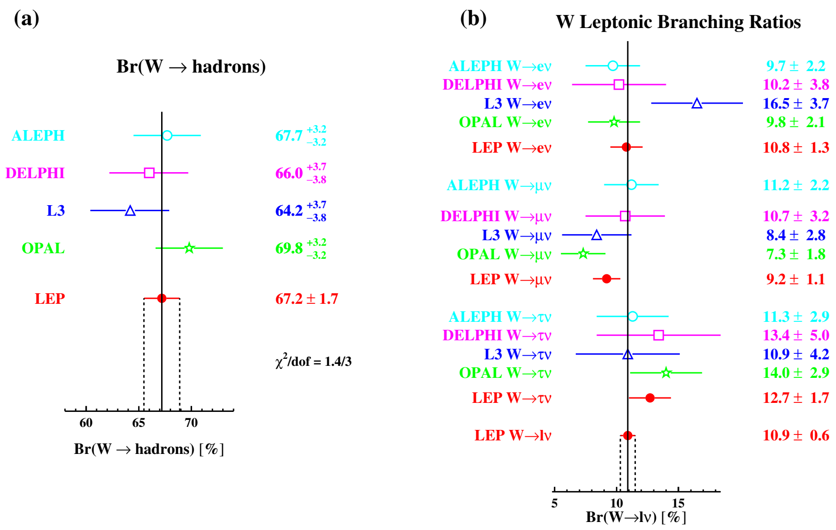

FIG. 6. The results of measurements on (a) WW branching fraction to hadron and (b) WW branching fraction to lepton. Each error on the measured values is the quadratic sum of statistical and systematic uncertainties.

$$\sum_{i=\mathrm{u,c};\, j=\mathrm{d,s,b}} |V_{ij}|^2 = 1.97 \pm 0.15. \tag{4}$$

This is consistent with a value of 2 which is expected from unitarity. Using the experimental knowledge [6] of the sum, $|V_{\mathrm{ud}}|^2 + |V_{\mathrm{us}}|^2 + |V_{\mathrm{ub}}|^2 + |V_{\mathrm{cd}}|^2 + |V_{\mathrm{cb}}|^2 = 1.05 \pm 0.01$, the above result can be interpreted as a measurement on $|V_{\mathrm{cs}}|$, the least well determined of these elements:

$$|V_{\mathrm{cs}}| = 0.96 \pm 0.08. \tag{5}$$

This result improves the determination of $|V_{\mathrm{cs}}|$ which do not invoke the unitarity constraint [6].

	$\mathrm{R_{cs}}$	$\mathrm{V_{cs}}$
ALEPH	$0.57 \pm 0.18 \pm 0.04$	$1.18 \pm 0.43 \pm 0.10$
DELPHI	$0.42 \pm 0.13 \pm 0.06$	$0.87 \pm 0.24 \pm 0.11$
Average	0.47 ± 0.11	0.95 ± 0.20

TABLE III. Direct measurements of the absolute value of the CKM matrix element $|\mathrm{V_{cs}}|$.

An additional piece of information can be obtained by tagging the flavour of jets produced in hadronic W decays. ALEPH and DELPHI directly measured $|V_{\mathrm{cs}}|$ by this method. ALEPH tagged charm decays with jet shape, energetic leptons and large impact parameters, and employed 12 variable neural network. Tagging the flavour of jets in the DELPHI detector is based on the measured impact parameters and particle identification. The results from both experiments together with the average of two experiments are shown in Table III. The results are consistent with the indirect measurements and the value expected from the unitarity. The direct measurements have rather large errors compared with the indirect measurement, but it is noticed that the results from direct measurements do not assume the Standard Model.

V. MASS OF W

With the precise measurement of the mass of the W boson at LEP2 the situation for electroweak input parameters changes with respect to LEP1. The common practice at LEP1 [8] is to use for M_{W} a value derived from the Fermi

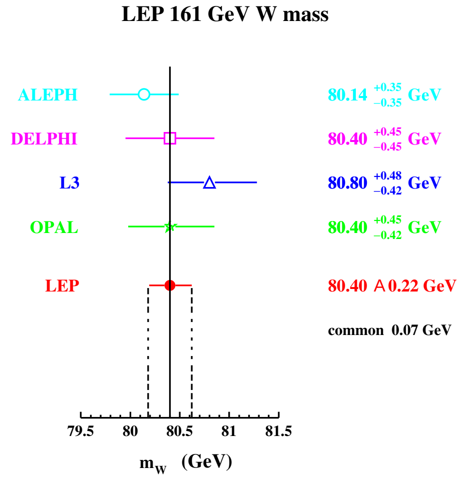

FIG. 7. The results of $M_{\rm W}$ measurements by W-pair cross-section at 161 GeV. Each error on the measured values is the quadratic sum of statistical and systematic uncertainties.

constant G_μ [6], which is accurately known from muon decay. The relation to obtain $M_{\rm W}$ follows from the Standard Model prediction for muon decay

$$G_\mu = \frac{\alpha\pi}{\sqrt{2}{M_{\rm W}}^2(1-{M_{\rm W}}^2/{M_{\rm Z}}^2)}\frac{1}{1-\Delta r}, \tag{6}$$

where $\Delta r = 0$ at tree level and where Δr is $m_{\rm t}$- and $M_{\rm H}$-dependent when loop corrections are included. Thus, $M_{\rm W}$ in LEP1 calculations is $m_{\rm t}$- and $M_{\rm H}$-dependent through the above procedure. At LEP2, where one wants to measure $M_{\rm W}$ and, hence, wants to treat $M_{\rm W}$ as a fit parameter, the above relation now primarily acts as a test of the Standard Model. The above relation predicts for any chosen $M_{\rm H}$ and measured $M_{\rm W}$ a value for $m_{\rm t}$ that can be used as input for LEP2 loop calculations and can also be compared with the directly observed top-quark mass from the Tevatron [17,18].

As to the actual procedure to measure $M_{\rm W}$ from W-pair production, two methods are advocated. One procedure requires a measurement of the total W-pair cross-section close to the threshold, where the size of $\sigma_{\rm tot}$ is most sensitive to the W mass. The other method looks at the decay products of the W boson and from the measured momenta of the decay products one tries to reconstruct the W mass.

A. W mass measurement by W-pair cross section

For an integrated $\mathcal{L}$ and an overall signal efficiency $\epsilon_{\rm WW} = \sum \epsilon_i BR_i$ (where the sum extends over the various channels selected, with branching ratios BR_i and efficiencies ϵ_i), the error on the $\rm W^+W^-$ cross-section due to signal statistics is given by

$$\Delta\sigma_{\rm WW} = \frac{\sigma_{\rm WW}}{\sqrt{N}} = \frac{\sqrt{\sigma_{\rm WW}}}{\sqrt{\epsilon_{\rm WW}\mathcal{L}}}, \tag{7}$$

where $N = \epsilon_{\rm WW}\sigma_{\rm WW}\mathcal{L}$ is the number of selected signal events. The corresponding error on the W mass is

$$\Delta M_{\rm W} = \sqrt{\sigma_{\rm WW}}\left|\frac{dM_{\rm W}}{d\sigma_{\rm WW}}\right|\frac{1}{\sqrt{\epsilon_{\rm WW}\mathcal{L}}}. \tag{8}$$

The sensitivity factor $\sqrt{\epsilon_{\rm WW}}|dM_{\rm W}/d\sigma_{\rm WW}|$ can be expressed as the function of $\sqrt{s}-2M_{\rm W}$. This function has a minimum at

$$(\sqrt{s})^{\rm opt} \simeq 2M_{\rm W} + 0.5{\rm GeV}, \tag{9}$$

corresponding to a minimum value of approximately 0.91 GeV pb$^{-1/2}$. This $(\sqrt{s})^{\rm opt}$ of 161 GeV is taken as the starting CME of LEP2. In the actual procedure of measuring the W mass by W-pair cross-section, equation 2 is employed again, where μ_i is given as a function of $M_{\rm W}$ and then the maximum likelihood value yields the measurement of the W mass. Fig.7 shows the results of W mass measurements by W-pair cross-section from four experiments together with the combined result.

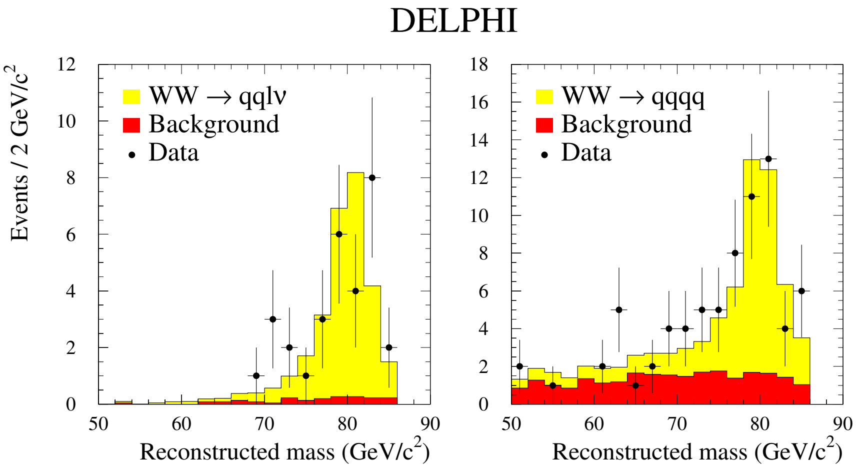

FIG. 8. Reconstructed invariant mass distributions for (a) semileptonic and (b) fully hadronic channels.

B. W mass measurement by direct reconstruction

At the CME of 172 GeV, the sensitivity of the W-pair production cross-section to the W mass is reduced, compared to the cross-section at threshold. Instead, at this higher energy, the measurement of the W mass can be made by direct reconstruction of the invariant mass of the fermion pairs from each W decay, using a kinematic fit technique with some constraints, which depends on different analysis methods and detector responses of four experiments. Incorporating the constraints of energy and momentum conservation into a kinematic fit significantly improves the invariant mass resolution and is adopted by all experiments. A specific combination of additional constraints and techniques, for example, a constraint of equal mass of two W bosons, a technique of beam energy rescaling and so on, is chosen by each experiment.

Events of the fully hadronic and semileptonic decay channels are used in the analysis. For each channel, several steps are needed to get the invariant mass distributions that are going to be used to extract the W mass. In the fully hadronic channel, four jets in an event can be divided into two di-jets in three different ways. It is not obvious which of these partitions is correct and so this ambiguity leads to a combinatorial background. Four experiments employed different pairing schemes to optimise the sensitivity to the W mass. OPAL, for example, performed three kinematic fits corresponding to the three combinations and placed an order with respect to the resulting fit probabilities. The combinations with the highest and second highest probabilities are used to extract the W mass information. In a $W^+W^-\to q\overline{q}\,l\overline{\nu}_l$ event (l =e or μ), a kinematic fit is performed including two jets and one lepton, imposing specific constraints of four experiments. For $W^+W^-\to q\overline{q}\tau\overline{\nu}_\tau$ events, ALEPH employed kinematic fits, L3 and OPAL utilised a technique of beam energy rescaling. Fig. 8 shows the distributions of the reconstructed invariant mass from DELPHI for (a) semileptonic and (b) fully hadronic channels, where a larger amount of background in fully hadronic channel than the semileptonic channel is due to the above mentioned jet-pairing combinatorial background.

The invariant mass distributions obtained from the event sample following the above procedures have a Breit-Wigner like shape but sizably distorted due to several effects such as phase space restrictions, detector resolution, initial state radiation, background contamination, selection algorithms, etc... Then a simple Breit-Wigner fit without corrections would not give the right answer to the W mass measurements. The most straightforward method to overcome this fact is using a simple Breit-Wigner fit, correcting the result and its actual uncertainty with proper calibration curves obtained from the study of the distortion using sets of Monte Carlo samples at different $M_{\rm W}$.

Nevertheless, to make a more optimal use of the information in the data, one would prefer to fit directly to the data the invariant mass distribution predicted by the Monte Carlo, which has our best knowledge of all the fore-mentioned distortions already folded in. Then a possible way of extracting the value of $M_{\rm W}$ from the data sample would be to generate a large number of Monte Carlo events for various input values of ${M_{\rm W}}^{MC}$ and find the best matching Monte Carlo sample to the data sample, where the ${M_{\rm W}}^{MC}$ of that Monte Carlo sample yields the measurement of $M_{\rm W}$. However, given the time required for full simulation of each event, generating such many Monte Carlo samples with different $M_{\rm W}$'s, which would correspond to a resolution for $M_{\rm W}$ measurement, is unfeasible in practice. To overcome this difficulty, an alternative approach is to generate a large amount of Monte Carlo events at just some specific values of M_{W} and weight them with the matrix element ratio

$$w_i(M_{\mathrm{W}},\Gamma_{\mathrm{W}}) = \frac{\left|\mathcal{M}(M_{\mathrm{W}},\Gamma_{\mathrm{W}},p_i^1,p_i^2,p_i^3,p_i^4)\right|^2}{\left|\mathcal{M}(M_{\mathrm{W}}^{MC},\Gamma_{\mathrm{W}}^{MC},p_i^1,p_i^2,p_i^3,p_i^4)\right|^2} \tag{10}$$

where $\mathcal{M}(M_{\mathrm{W}},\Gamma_{\mathrm{W}},p_i^1,p_i^2,p_i^3,p_i^4)$ is the matrix element of the process

$$\mathrm{e}^+\mathrm{e}^- \to W^+W^- \to f_1\bar{f}_2f_3\bar{f}_4 \tag{11}$$

where p_i^j denotes the 4-momentum of the outgoing fermion j for a particular event i. The matrix element $\mathcal{M}$ is evaluated for the CC03 diagrams. This weighting method enables one to obtain a Monte Carlo sample with an arbitrary input value of M_{W} from the generated Monte Carlo samples with some specific values of M_{W}. ALEPH, L3 and OPAL employed this weighting method to extract the W mass.

On the other hand, DELPHI developed a different method in which the information on the W mass is extracted from the likelihood of observing each individual event. For example, in the case of semileptonic candidates, the likelihood is expressed as:

$$\mathcal{L}(M_{\mathrm{W}}) = P\left(\int_0^{E_b} G(m|m_{\mathrm{f}})BW(m|M_{\mathrm{W}})PS(m)dm\right) + (1-P)p_b(m_{\mathrm{f}}), \tag{12}$$

where P is the overall fraction of events expected from simulation to be signal (90% for the electron events and 98% for the muon events). $G(m|m_{\mathrm{f}})$ is a Gaussian resolution function:

$$G(m|m_{\mathrm{f}}) = \frac{1}{\sqrt{2\pi}\sigma_{\mathrm{f}}}\exp\left(-\frac{(m-m_{\mathrm{f}})^2}{2\sigma_{\mathrm{f}}^2}\right), \tag{13}$$

where m_{f} is the value of the fitted invariant mass and σ_{f} is the error on m_{f}. $BW(m|M_{\mathrm{W}})PS(m)$ is the expected distribution of the average of two W masses:

$$BW(m|M_{\mathrm{W}})PS(m) \propto \frac{\Gamma_{\mathrm{W}}}{M_{\mathrm{W}}}\frac{m^2}{(m^2-M_{\mathrm{W}}^2)^2 + m^4\Gamma_{\mathrm{W}}^2/M_{\mathrm{W}}^2}\sqrt{E_b^2-m^2}, \tag{14}$$

where the width of the W resonance is taken as $\Gamma_{\mathrm{W}} = 2.07$ GeV. The shape of the background distribution, $p_b(m_{\mathrm{f}})$, is taken numerically from simulation.

For fully hadronic events, the expression is more involved due to the jet-pairing, where DELPHI treated not only 4-jet candidates but also 5-jet ones where 10 combinations of jet-pairing are possible. In the case of 4-jet events, the relative probability which gives the correct jet-pairing probability is estimated for all jet combinations. For the 5-jet candidates, each of the ten relative probabilities is determined with gluon radiation being taken into account. In addition, the efficiencies of the jet reconstruction are estimated for 4-jet and 5-jet events. All of these estimates are included in the expression of the likelihood for observing a fully hadronic event.

It is noticed that the likelihood mentioned above is determined for an event. The combined likelihood for observing all the events is expressed as the product of all the event likelihoods. The maximum of this combined likelihood then yields the measurement of the W mass.

Fig. 9 shows the results of W mass measurement by direct reconstruction for (a) semileptonic and (b) fully hadronic channels. The LEP combined results of both channels are shown in Fig. 10. The systematic uncertainties affecting the results are studied by all experiments. For example, main part of the systematic error studies by ALEPH is described here. The systematic error coming from Monte Carlo statistics is estimated to be $\Delta\ M_{\mathrm{W}} = 30$, 35 and 90 MeV for the hadronic, $e\mu$ and τ channels respectively. The matrix element used in this analysis corresponds to the CC03 diagrams instead of the complete matrix element which includes all possible diagrams. This effect is estimated to be $\Delta\ M_{\mathrm{W}} = 3$ MeV on the M_{W}. Errors from detector mis-calibration are quated as $\Delta\ M_{\mathrm{W}} = 40$, 60 and 106 MeV for the hadronic, $e\mu$ and τ channels respectively. ISR effect and LEP beam energy error constribute 15 and 30 MeV, respectively, in all channels. Uncertainties from colour reconnection and Bose-Einstein effects are quated as 50 and 40 MeV in hadronic channel only. In total, systematic errors of 100, 120 and 170 MeV for the hadronic, $e\mu$ and τ channels, respectively, are obtained in the studies by ALEPH.

The W mass measurements at the threshold and higher energies together with other precise electroweak measurements performed at LEP are used to check the validity of the Standard Model and, within its framework, to infer valuable information about its fundamental parameter, in paticular the top-quark mass, m_{t}, and Higgs boson mass,

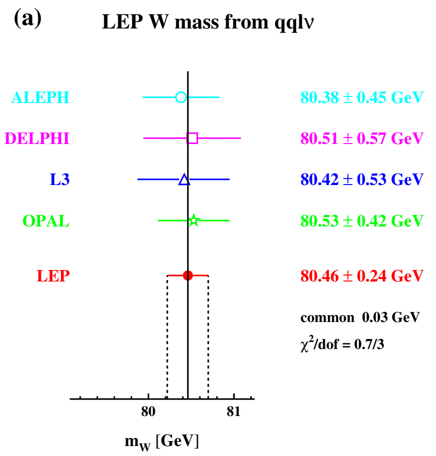

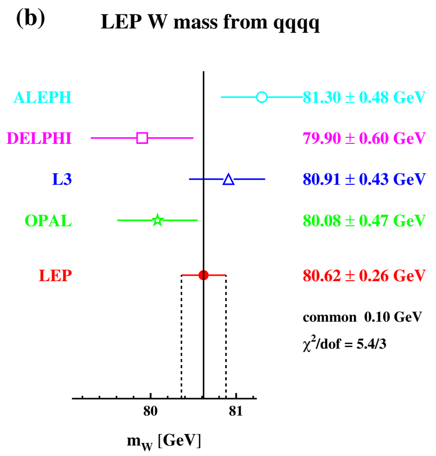

FIG. 9. The results of W mass measurements by direct reconstruction for (a) semileptonic and (b) fully hadronic channels. Each error on the measured values is the quadratic sum of statistical and systematic uncertainties.

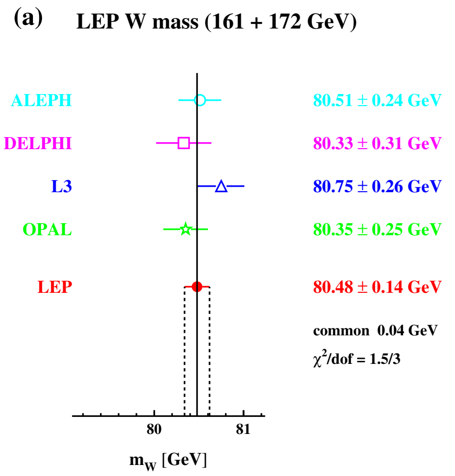

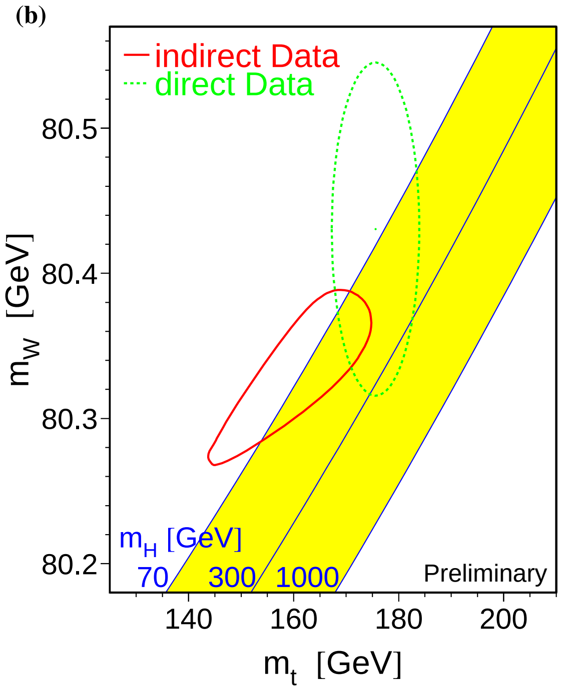

FIG. 10. (a) the LEP combined result of W mass measurements by cross-section measurement and direct reconstruction, where each error on the measured values is the quadratic sum of statistical and systematic uncertainties, and (b) the comparison of the indirect measurements of m_W and m_t (LEP+SLD+νN data) (solid contour) and the direct measurements (Tevatron and LEP2 data) (dashed contour). In both cases the 68% C.L. contours are plotted. Also shown is the Standard Model relationship for the masses as a function of the Higgs mass.

$M_{\rm H}$. In this procedure, to obtain the best sensitivity also used are: the results from SLD [9] as well as measurements of $M_{\rm W}$ from UA2 [10], CDF [11,12], and DØ [13], measurements of the neutrino neutral to charged current ratios from CDHS [14], CHARM [15] and CCFR [16], and measurement of the top quark mass [17–19] by CDF and DØ. The combined results excepting the LEP2 and Tevatron $M_{\rm W}$ and $m_{\rm t}$ determine the top quark and W masses indirectly, and are compared to the direct measurements performed at the Tevatron and LEP. This comparison and the Standard Model predicions for Higgs masses between 60 and 1000 GeV are shown in Fig. 10 (b). As can be seen in figure, the indirect measurements prefer low $m_{\rm t}$ and low $M_{\rm H}$. The best constraints on $M_{\rm H}$ is obtained when all data are used in the fit. The result of this fit is $M_{\rm H}= 115^{+116}_{-66}$ GeV.

VI. TRIPLE GUAGE-BOSON COUPLINGS

The $\rm W^+W^-$production process involves the triple gauge-boson vertices between the $\rm W^+W^-$ and the $\rm Z^0$ or photon. All evidence for the existence of triple gauge-boson vertices and measurements of the Triple Gauge-boson Couplings (TGC) has, until now, been indirect or is based on estimate from high energy $\rm p\bar{p}$ collisions [20]. The measurement of these Triple Gauge-boson Couplings (TGCs) and the search for possible anomalous values in the very clean envirnment of $\rm e^+e^-$collisions is one of the principal physics goals at LEP2.

The most general Lorentz invariant Lagrangian [21–25] which describes the triple guage-boson interaction has up to fourteen independent terms, seven describing the WWγ vertex and seven describing the WWZ vertex. This parameter space is very large, and it is not currently possible to measure all fourteen couplings independently. Assuming electromagnetic gauge invariance and C and P conservation the number of parameters reduces to five, which we can write as $g_1^{\rm Z}$, $\kappa_{\rm Z}$, κ_γ, $\lambda_{\rm Z}$ and λ_γ following the notation used in [21,22]. In the Standard Model $g_1^{\rm Z} = \kappa_{\rm Z} = \kappa_\gamma = 1$ and $\lambda_{\rm Z} = \lambda_\gamma = 0$.

The TGCs contribute, via loop corrections, to obsevables which can be measured at LEP1 and there has been a rich discussion on the bounds in the parameter space that can be deduced from the huge amount of LEP1 precision data [26,27]. To parameterise the so-called "blind directions" in the multidimensional space of TGCs where the constraints from LEP1 analyses are very weak, three linear combination of these couplings have been proposed [21–23]. The three TGCs, $\alpha_{{\rm W}\phi}$, $\alpha_{\rm W}$, and $\alpha_{{\rm B}\phi}$, introduced to parametrise these linear combinations form the most general set of TGCs which can be embedded into an theory that preserve local $\rm SU(2)_{\mathit{L}}\times U(1)_{\mathit{Y}}$ invariance. In terms of the notation in [21] they are

$$\begin{aligned}\alpha_{{\rm W}\phi} &= \Delta g_1^{\rm Z}\cos^2\theta_w \\ \alpha_{\rm W} &= \lambda_\gamma \\ \alpha_{{\rm B}\phi} &= \Delta\kappa_\gamma - \Delta g_1^{\rm Z}\cos^2\theta_w\end{aligned} \tag{15}$$

along with constraints $\Delta\kappa_{\rm Z} = \Delta g_1^{\rm Z} - \Delta\kappa_\gamma \tan^2\theta_w$ and $\lambda_\gamma = \lambda_{\rm Z}$. The Δ denotes the deviations of the respective quantity from its non-zero Standard Model value and θ_w is the weak mixing angle. In this analysis the couplings $\alpha_{{\rm W}\phi}$, $\alpha_{\rm W}$ and $\alpha_{{\rm B}\phi}$ are measured individually assuming the two other couplings to be fixed at zero, their Standard Model expectation.

A. Experimental variables

The important kinematic quantities for TGC measurements in $\rm W^+W^-$ events are the five variables:

- $\cos\Theta_{\rm W}$, the production polar angle of the $\rm W^-$ boson.
- $\cos\theta^*_{-,+}$, the polar decay angle of the charged lepton or down type quark with respect to the flight direction of the $\rm W^{-,+}$, measured in its rest frame.
- $\phi^*_{-,+}$, the azimuthal decay angle of the the charged lepton or down type quark with respect to the plane defined by the direction of $\rm W^{-,+}$ and the incoming electron.

The total cross-section of W-pair production is sensitive to the TGCs, but the differential cross-section:

$$d\sigma = d\sigma(\Omega) \tag{16}$$

$$\Omega = (\Theta_{\rm W}, \theta^*_{-,+}, \phi^*_{-,+}) \tag{17}$$

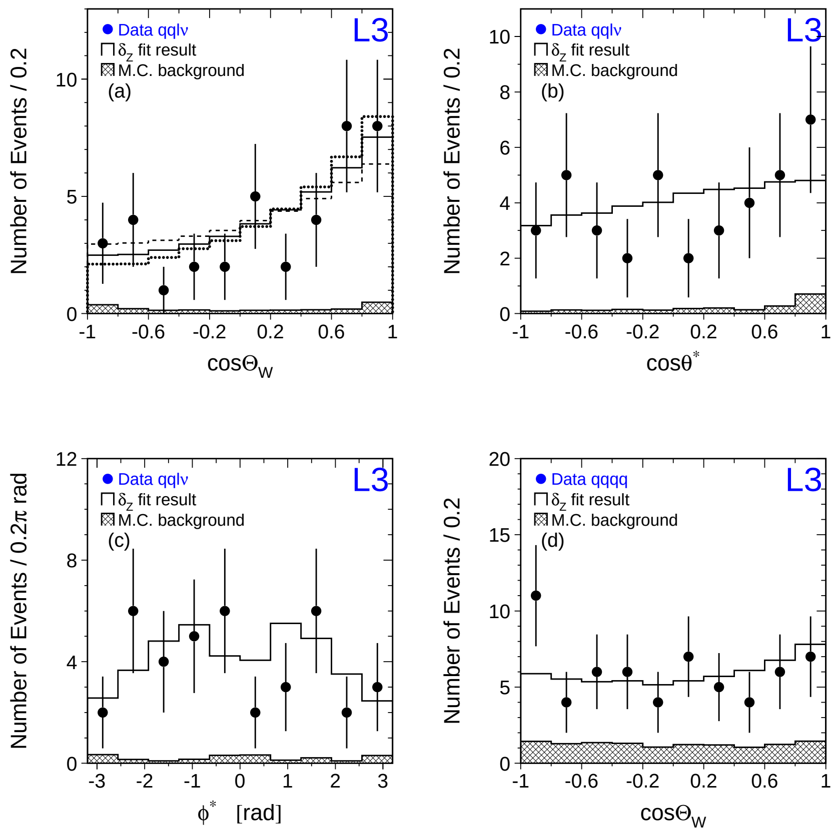

FIG. 11. Distribution of reconstructed phase-space angles after applying the kinematic fit using the equal-mass constraint. (a) The polar angle of the W^- boson, $\cos\Theta_W$, for selected $q\bar{q}l\bar{\nu}_l$ events. (b) The polar decay angle of the leptonically decaying W boson, $\cos\theta^*$, for selected $q\bar{q}l\bar{\nu}_l$ events. (c) The azimuthal decay angle of the leptonically decaying W boson, ϕ^*, for selected $q\bar{q}l\bar{\nu}_l$ events. The value of ϕ^* is shifted by π for W^- decays in order to have the same ϕ^* distribution for W^- and W^+ decays. (d) The polar angle of the W^- boson, $\cos\Theta_W$, for selected $q\bar{q}q\bar{q}$ events.

contains more pieces of information on TGCs. As a first step to extract the information on TGCs from $\sigma(\Omega)$, the momenta and energies of the decay products from W bosons are measured and fed into the kinematic fits which improve the resolution of the measurements of the five variables. For semileptonic events the charge of the reconstructed lepton together with the two jets determines the W^- direction and hence allows for unambiguous determination of the primary variable for measurement of the TGCs, the W^- boson production angle. The $\cos\theta^*$ and ϕ^* in the leptonic system are also measured clearly. For hadronic jets, the flavour and charge of the original quark is not measured. Thus, there arises a two-fold ambiguity in the decay angles of hadronically decaying W bosons, $(\cos\theta^*, \phi^*) \leftrightarrow (-\cos\theta^*, \pi+\phi^*)$. If both W boson decay hadronically, the polar angle of the W^- boson also has a two-fold ambiguity, $\cos\Theta_W \leftrightarrow -\cos\Theta_W$. This ambiguity is resolved by combining the jet charges of each pair of jets to determine the charge of each W. The difference in the two W charges is then used to determine the sign of $\cos\Theta_W$. For example, L3 determines the charge of each jet from a rapidity weighted sum of the tracks reconstructed in the central tracking chamber and assigned to the jet with rapidity weight $\kappa = 1.0$ [28]. The sign assignment is found to be correct 67% of the time when the jets are correctly paired. The distributions of these phase-space angles from L3 are shown in Fig. 11.

B. Extraction of TGCs

Several methods to extract anomalous couplings have been investigated in order to evaluate their sensitivity to the TGCs. As the result, all four experiments employed methods utilising so-called 'Optimal Observables' (OO) which project the relevant kinematical information sensitive to a certain TGC onto a one dimensional distribution [29]. If the differential cross-section $d\sigma/d\Omega$ is expanded as a function of a TGC α:

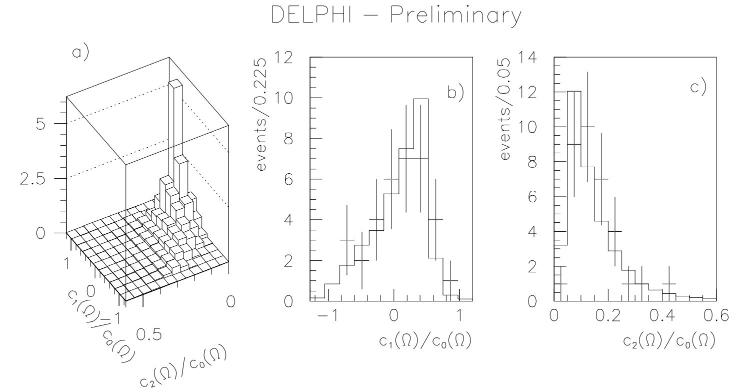

FIG. 12. a) Distribution of $C_1(\Omega)/C_0(\Omega)$ versus $C_2(\Omega)/C_0(\Omega)$ for $\alpha_{W\phi}$ for 172 GeV data in the semileptonic channel. b) Projection onto the $C_1(\Omega)/C_0(\Omega)$ axis. c) Projection onto the $C_2(\Omega)/C_0(\Omega)$ axis. The points in b) and c) represent the data, and the histograms the expectation for the fitted value of $\alpha_{W\phi}$.

$$\frac{d\sigma}{d\Omega}(\alpha) = C_0(\Omega) + \alpha C_1(\Omega) + \alpha^2 C_2(\Omega), \tag{18}$$

and it is differentiated by the TGC α as:

$$\frac{1}{C_0(\Omega)}\frac{d}{d\alpha}\frac{d\sigma}{d\Omega} = \frac{C_1(\Omega)}{C_0(\Omega)} + 2\alpha\frac{C_2(\Omega)}{C_0(\Omega)}, \tag{19}$$

the distributions of 2-variable space $(C_1/C_0, C_2/C_0)$ retains the whole information on a single parameter α. Thus a fit to $(C_1/C_0, C_2/C_0)$ allows the determination of a parameter α with maximum precision. For example, DELPHI analysed data at 172 GeV by performing a binned extended maximum likelihood fit to two-dimensional distribution of $(C_1/C_0, C_2/C_0)$ for each TGC parameter, where total cross-section information is also included. Fig. 12 shows the distribution of the data in the $(C_1/C_0, C_2/C_0)$ plane, together with its projections onto the two axes and the expected distributions for the fitted value of one TGC parameter, $\alpha_{W\phi}$.

Fig. 13 (a), (b) and (c) show the results of the three TGCs, $\alpha_{W\phi}$, α_W and $\alpha_{B\phi}$, respectively, where each error on the measured couplings is the quadratic sum of statistical and systematic uncertainties. As seen in the figure, the LEP combined results of three TGCs are obtained each by adding likelihood curves of four experiments. These combined results are in good agreement with the Standard Model prediction. Systematic uncertainties are determined by modifying the Monte Carlo simulation for the effect under study. For example, the estimates of the uncertainties by ALEPH are described here. The largest component of the systematic uncertainties is the effect of the colour reconnection. This is amounted approximately 40% of the statistical uncertainties. The other main components are from fragmentation, jet reconstruction and initial state radiation. The changes of TGCs by these sources are typically 20% of the statistical uncertainties. In total, the systematic uncertainties amounted to 40%, 20% and 20% of the statistical uncertainties for $\alpha_{W\phi}$, α_W and $\alpha_{B\phi}$, respectively.

VII. W HADRONIC DECAY PROPERTIES

A. Colour reconnection effects

It has been shown that [30,31] the average charge multiplicities and single particle distributions of the fully hadronic channel are sensitive to colour reconnection effects. These approaches predict that colour reconnection effects at 172 GeV in fully hadronic events lead to a smaller average charged particle multiplicity compared to twice the multiplicity of semileptonic events:

$$\frac{< N_{ch}^{4\mathrm{q}} >}{2 < N_{ch}^{\mathrm{qqln}} >} \; < \; 1. \tag{20}$$

Therefore, the quantity $\Delta < N_{ch} > = < N_{ch}^{4\mathrm{q}} > - \, 2 < N_{ch}^{\mathrm{qqln}} >$ is measured. Results from DELPHI, L3 and OPAL are shown in Table IV, where no significant discrepancy from zero is observed in $\Delta < N_{ch} >$ measurements.

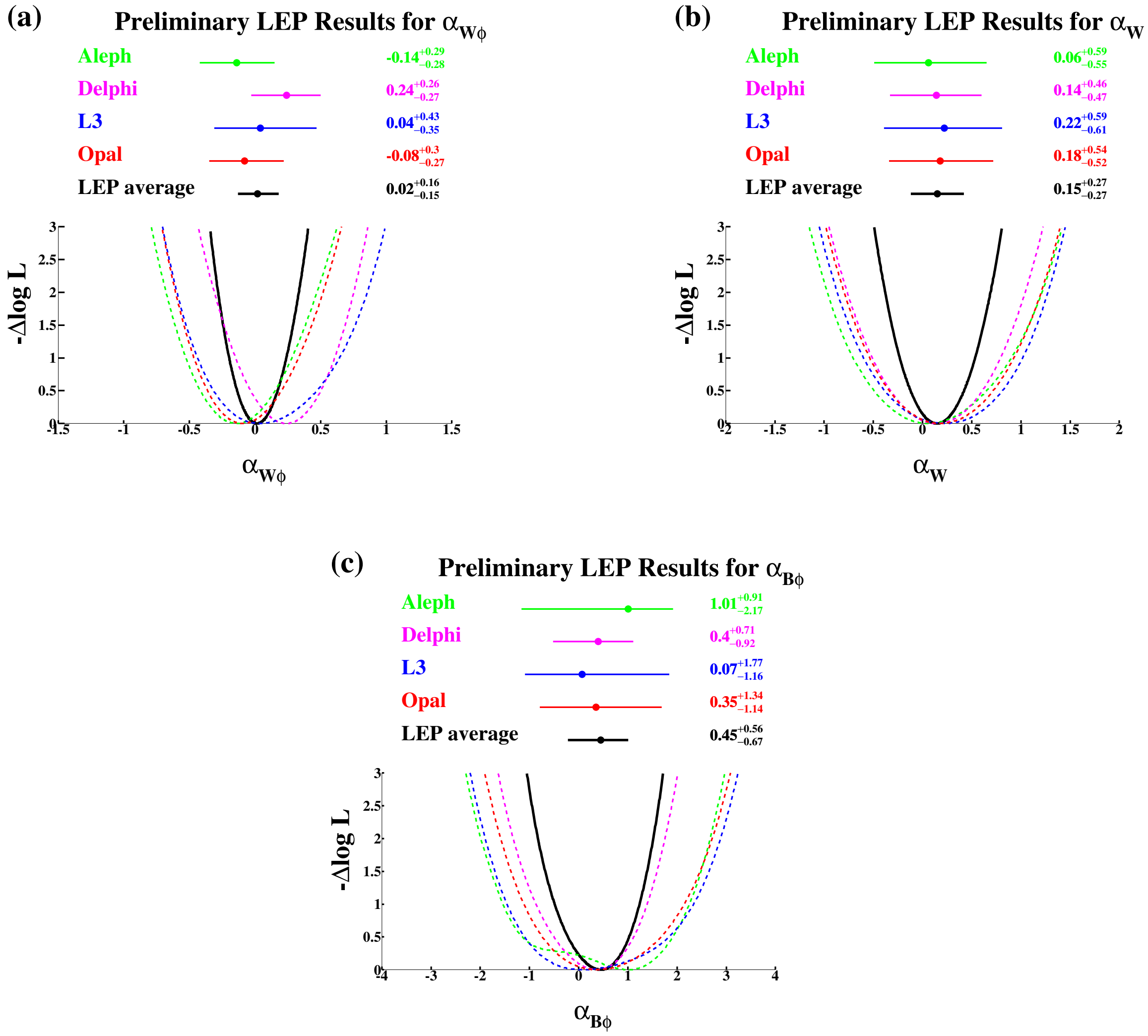

FIG. 13. The results of measurements on three TGCs, (a) $\alpha_{\mathrm{W}\phi}$, (b) α_{W} and (c) $\alpha_{\mathrm{B}\phi}$, where each error is the quadratic combination of statistical and systematic uncertainties.

	$N_{ch}^{4\mathrm{q}}$	N_{ch}^{qqln}	N_{ch}^{qqln}
DELPHI	41.7 ± 1.8	36.4 ± 2.2	$+5.3 \pm 2.8$
L3	37.9 ± 0.9	38.8 ± 1.2	-0.9 ± 1.5
OPAL	$38.3 \pm 1.1 \pm 0.6$	$36.8 \pm 1.8 \pm 0.8$	$+1.5 \pm 2.2 \pm 0.8$

TABLE IV. Results of ΔN_{ch} measurements from DELPHI, L3 and OPAL. The first errors are statistical and the second errors of OPAL are systematic.

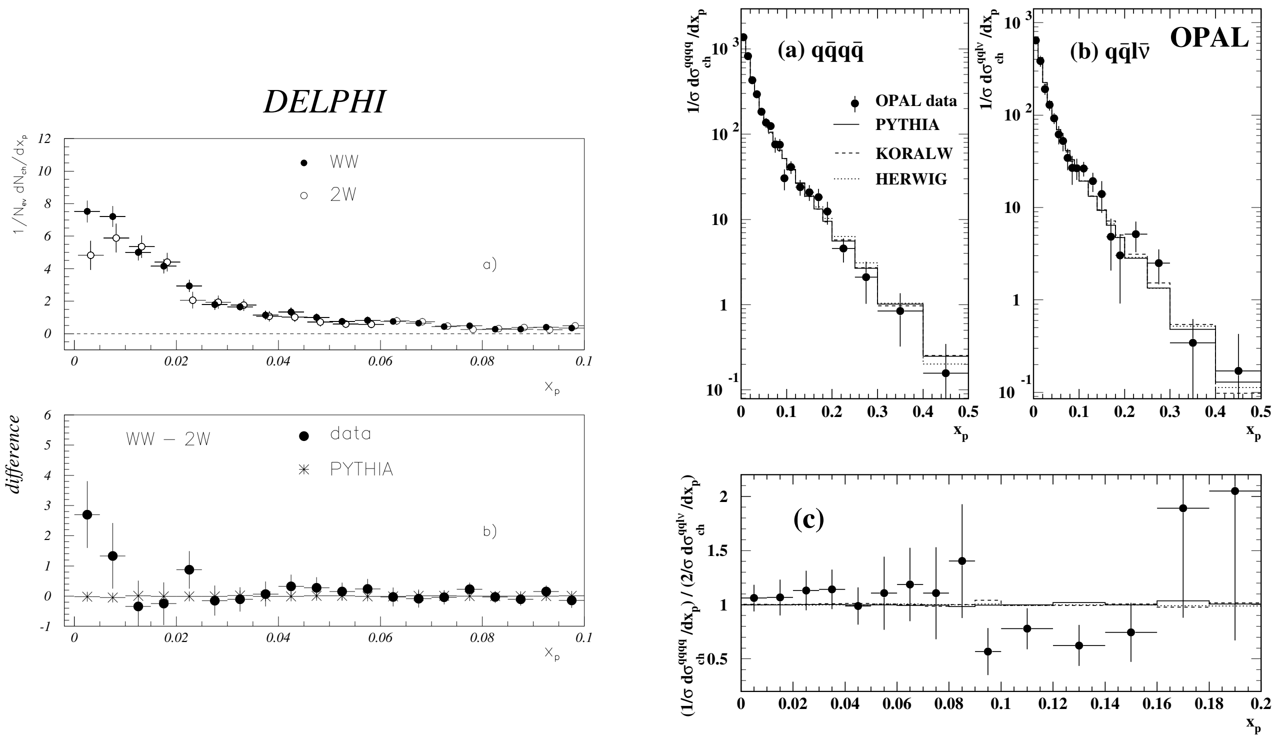

FIG. 14. (a) in the left-hand side: the corrected x_p distributions for charged particles from hadronic W-decays for fully hadronic final states (closed circles) and twice the semileptonic final states (open circles), from DELPHI. The distributions are normalised to the number of events. (b) in the left-hand side: the difference between the distributions of (a), from DELPHI. The predicted difference obtained by using events generated with PYTHIA is shown by stars. (a) in the right-hand side: corrected x_p distributions for $W^+W^- \to q\overline{q}q\overline{q}$ events from OPAL. (b) in the right-hand side: the hadronic part of $W^+W^- \to q\overline{q}\,l\overline{\nu}_l$ events and (c) the ratio of the $W^+W^- \to q\overline{q}q\overline{q}$ distribution to twice the $W^+W^- \to q\overline{q}\,l\overline{\nu}_l$ distribution, from OPAL. The points indicate the data, with statistical and systematic uncertainties added in quadrature, and the predictions of various Monte Carlo models (without colour reconnection) are shown as histograms.

A reduction of charged particle multiplicities (i.e. single particle distribution) in fully hadronic decay channel is expected particularly in the low momentum region, $p < 1$ GeV/c [30]. Thus the quantity $\Delta < x_p > = < x_p^{4q} > - 2 < x_p^{\mathrm{qqln}} >$ is also examined, where $x_p \equiv p/\sqrt{s}$. The distributions of $< x_p >$ and $\Delta < x_p >$ from DELPHI and OPAL are shown in Fig. 14. The distributions of $\Delta < x_p >$ from DELPHI show an excess at low momentum region. On the other hand, the distributions of $\Delta < x_p >$ from OPAL show no excess at the same region. Thus, more data at higher energies are needed to search, or confirm the observation of the colour reconnection effects at the low momentum region of single particle distributions.

B. Bose-Einstein correlations

The Bose-Einstein effect is a positive correlation in narrow momentum space among identical bosons produced in the hadronization process. The correlations were studied in the hadronic decays of the Z^0 at LEP1 [32,33], where a strong effect was observed. It has also been conjectured that the measurement of the W mass at LEP2 using fully hadronic 4-jet events is likely to be affected by Bose-Einstein correlations between pions from different Ws [34]. Recent studies [35] using Monte Carlo generators implemented with Bose-Einstein correlations reported that the effect on the measurements of W mass may be less than 20 MeV.

ALEPH and DELPHI studied Bose-Einstein correlations between pions from different Ws in e^+e^- annihilations at 172 GeV, by comparing the semileptonic and fully hadronic W-pair decays. Here the simplest method of analysing of

	$W^+W^-\to q\overline{q}\,l\overline{\nu}_l$	$W^+W^-\to q\overline{q}q\overline{q}$
ALEPH	$\lambda = 0.96 \pm 0.84$ $\sigma = 0.99 \pm 0.41$ fm	$\lambda = 0.12 \pm 0.12$ $\sigma = 0.64 \pm 0.38$ fm
DELPHI	$\lambda = 0.41 \pm 0.13$ $\sigma = 0.5$ fm fixed	$\lambda = 0.09 \pm 0.06$ $\sigma = 0.5$ fm fixed

TABLE V. The results of fits with parameters λ: the strength of the correlation, and σ: the source radius, to $R^*(Q)$ distributions of $W^+W^-\to q\overline{q}q\overline{q}$ and $W^+W^-\to q\overline{q}\,l\overline{\nu}_l$ event data at 172 GeV.

Bose-Einstein correlations is used: the comparison of like-sign pair and unlike-sign pair of charged particle distributions as a function of $Q = \sqrt{(P_1 - P_2)^2 - (E_1 - E_2)^2}$, where P_i and E_i are the 3-momenta and energies of particle i, respectively. Therefore, the correlation function $R(Q)$ is defined as

$$R(Q) = \frac{\pi^{++,--}(Q)}{\pi^{+-}(Q)} \tag{21}$$

where $\pi^{++,--}(Q)$ and $\pi^{+-}(Q)$ are unlike-sign and like-sign Q distributions of pions, respectively. In ALEPH analysis, the $R^*(Q)$ distributions are obtained by dividing the data distribution by the Monte Carlo one in order to correct for the effect of acceptance and resonance decay products. This distribution is fitted with the formula from [32]:

$$R^*(Q) = \kappa(1+\epsilon Q)(1+\lambda \exp(-\sigma^2 Q^2)) \tag{22}$$

where the parameter σ gives the source radius and λ the strength of the correlation between pions. The fits are performed with both hadronic and semileptonic W-pair event data at 172 GeV. DELPHI also performed similar fits to data at 172 GeV. Both results are shown in in Table V, where the correlation strength λ's of semileptonic events are consistent with the reported values in [32] ($\lambda = 0.40 \pm 0.02$) and [33] ($\lambda = 0.35 \pm 0.04$) from Z^0 data, and are higher than the strength of fully hadronic events. In order to measure the Bose-Einstein correlations between pions from different W in the fully hadronic channel, ALEPH made the $R^{**}(Q)$ distribution using formula

$$R^{**}(Q) = \left(\frac{N\pi_{4q}^{++,--} - 2N\pi_{qqln}^{++,--}}{N\pi_{4q}^{+-} - 2N\pi_{qqln}^{+-}}\right)^{data} / \left(\frac{N\pi_{4q}^{++,--} - 2N\pi_{qqln}^{++,--}}{N\pi_{4q}^{+-} - 2N\pi_{qqln}^{+-}}\right)^{MC}. \tag{23}$$

The result is that the data favour the absence of Bose-Einstein correlations between pions from different Ws, but their existence cannot be ruled out, even at 1 σ level. DELPHI experiment also investigated the Bose-Einstein correlations between identical pions from different Ws in $W^+W^-\to q\overline{q}q\overline{q}$ events. Conclusions from two experiments are summarised here: at present level of statistical precision, no enhancement of the correlation function is observed at small Q values in the measurements of the correlation function for like-sign particles arising from different Ws in fully hadronic channel.

VIII. SUMMARY

LEP2 started successfully at the energy just above the W-pair production threshold and raised the energy to significantly above the threshold. At both energies it enabled the four experiments, ALEPH, DELPHI, L3 and OPAL to study the physics on W-pair production in very clean environment of e^+e^-collisions. The main combined results of four experiments are, W-pair cross-section: $\sigma_{WW}= 3.69 \pm 0.45$ pb at 161 GeV and $\sigma_{WW}= 11.96 \pm 0.70$ pb at 172 GeV, W-pair branching fraction: $Br(W \to \text{hadron}) = 67.2 \pm 1.7\%$ and $Br(W \to \text{lepton}) = 10.9 \pm 0.6\%$, improvement on CKM matrix element: $|V_{CS}| = 0.96 \pm 0.08$, mass of W: $M_W= 80.48 \pm 0.14$ GeV, and three TGCs: $\alpha_{W\phi}= 0.02^{+0.16}_{-0.15}$, $\alpha_W= 0.15^{+0.27}_{-0.27}$ and $\alpha_{B\phi}= 0.45^{+0.56}_{-0.67}$. In addition, colour reconnection and Bose-Einstein effects are investigated in fully hadronic channel, where at present level of statistical precision, none of both effects originated from different Ws was observed. All the obtained results are in excellent agreement with the Standard Model expectations.

IX. ACKNOWLEDGEMENTS

We wish to congratulate the CERN accelerator divisions for the successful upgrade of the LEP machine, its good performance and careful work on the beam energy determination. We also acknowledge with appreciation the effort of all engineers, technicians and support staff who have participated in the construction and maintenance of four experiments: ALEPH, DELPHI, L3 and OPAL. At last, but not least, we are grateful to our funding agencies for their continuing support.

---

[1] ALEPH Collaboration, Nucl. Instrum. Meth. **A294** (1990) 121; ALEPH Collaboration, Nucl. Instrum. Meth. **A360** (1995) 481.
[2] DELPHI Collaboration, Nucl. Instrum. Meth. **A303** (1991) 233; DELPHI Collaboration, Nucl. Instrum. Meth. **A378** (1996) 57.
[3] L3 Collaboration, Nucl. Instrum. Meth. **A289** (1990) 35; M. Chemarin *et al.*, Nucl. Instrum. Meth. **A349** (1994) 345; M. Acciarri *et al.*, Nucl. Instrum. Meth. **A351** (1994) 300; G. Basti *et al.*, Nucl. Instrum. Meth. **A374** (1996) 293; I. C. Brock *et al.*, Nucl. Instrum. Meth. **A381** (1996) 236; A. Adam *et al.*, Nucl. Instrum. Meth. **A383** (1996) 342.
[4] OPAL Collaboration, Nucl. Instrum. Meth. **A305** (1991) 275; P. P. Allport *et al.*, Nucl. Instrum. Meth. **A324** (1993) 34; P. P. Allport *et al.*, Nucl. Instrum. Meth. **A346** (1994) 476.
[5] T. Sjöstrand, PYTHIA 5.7 / JETSET 7.4, CERN-TH.7112/93 (1993).
[6] The Particle Data Group, R. M. Barnett *et al.*, Phys. Rev. **D54** (1996) 1.
[7] Proceedings of CERN LEP2 Workshop, CERN 96-01, Vols. 1 and 2, eds. G. Altarelli, T. Sjöstrand and F. Zwirner, February 1996.
[8] D. Bardin, W. Hollik and G. Passarino (eds.), *Reports of the working group on precision calculations for the Z resonance* (CERN-95-03, Geneva, 1995).
[9] SLD Collaboration, P. Rowson, talk presented at Moriond 97.
[10] UA2 Collaboration, J. Alitti *et al.*, Phys. Lett. **B276** (1992) 354.
[11] CDF Collaboration, F. Abe *et al.*, Phys. Rev. Lett. **65** (1990) 2243 and Phys. Rev. **D43** (1991) 2070.
[12] CDF Collaboration, F. Abe *et al.*, Phys. Rev. Lett. **75** (1995) 11 and Phys. Rev. **D52** (1995) 4784;
A. Goldon, talk presented at XXXIInd Rencontres de Moriond, Les Arcs, 16-22 March 1997, to appear in the proceedings.
[13] DØ Collaboration, S. Abachi *et al.*, Phys. Rev. Lett. **77** (1996) 3309;
K. Streets, talk presented at Hadron Collider Physics 97, Stony Brook, to appear in the proceedings.
[14] CDHS Collaboration, H. Abramowicz *et al.*, Phys. Rev. Lett. **57** (1986) 298; CDHS Collaboration, H. Blondel *et al.*, Z. Phys. **C45** (1990) 361.
[15] CHARM Collaboration, J. V. Allaby *et al.*, Phys. Lett. **B177** (1986) 446; CHARM Collaboration, J. V. Allaby *et al.*, Z. Phys. **C36** (1987) 611.
[16] CCFR Collaboration, K. McFarland, *A Precision Measurement of Electroweak Parameters in Neutrino-Nucleon Scattering*, FERMILAB-PUB-97/001-E, January 1997, submitted to Phys. Rev. Lett.
[17] CDF Collaboration, J. Lys, talk presented at ICHEP96, Warsaw, 25-31 July 1996, to appear in the proceedings.
[18] DØ Collaboration, S. Protopopescu, talk presented at ICHEP96, Warsaw, 25-31 July 1996, to appear in the proceedings.
[19] The CDF and DØ results have been averaged together assuming a 3 GeV common systematic error.
[20] CDF Collaboration, F. Abe *et al.*, Phys. Rev. Lett. **75** (1995) 1017;
DØ Collaboration, S. Abachi *et al.*, Phys. Rev. Lett. **75** (1995) 1023, S. Abachi *et al.*, Phys. Rev. Lett. **77** (1996) 3303.
[21] Physics at LEP2, Edited by G. Altarelli, T. Sjöstrand and F. Zwirner, Report on the LEP2 workshop 1995, CERN 96-01 (1996) Vol. 1 p525.
[22] K. Hagiwara, R. Peccei, D. Zeppenfeld and K. Hikasa, Nucl. Phys. **B282** (1987) 253.
[23] M. Bilenky, J. L. Kneur, F. M. Renard and D. Schildknecht, Nucl. Phys. **B409** (1993) 22.
[24] M. Bilenky, J. L. Kneur, F. M. Renard and D. Schildknecht, Nucl. Phys. **B419** (1994) 240.
[25] K. Gaemers and G. Gounaris, Z. Phys. **C1** (1979) 259.
[26] A. De Rújula, M. B. Gavela, O. Pène and F. J. Vegas, Nucl. Phys. **B357** (1991) 311.
[27] A. De Rújula, M. B. Gavela, P. Hernandez and E. Massó, Nucl. Phys. **B384** (1992) 3.
[28] R. D. Field, R. P. Feynman, Nucl. Phys. **B136** (1978) 1.
[29] M. Diehl and O. Nacthmann, Zeit. Phys. **C62** (1994) 397.
[30] T. Sjöstrand and V. A. Khoze, Zeit. Phys. **C62** (1994) 281.
[31] J. Ellis and K. Geiger, "Signatures of Parton Exogamy in $e^+e^- \to W^+W^- \to$ *hadrons*", CERN-TH/97-46.
[32] ALEPH Collaboration, D. Decamp *et al.*, Zeit. Phys. **C54** (1994) 75.
[33] DELPHI Collaboration, P. Abreu *et al.*, Phys. Lett. **B286** (1992) 201.
[34] L. Lönnblad and T. Sjöstrand, Phys. Lett. **B351** (1995) 293.
[35] S. Jadach and K. Zalewski, CERN-TH/97-29: V. Kartvelishvili, R. Kvatadze, R. Moller hep-ph/9704424, 28/4/97.